

Available online at [www.sciencedirect.com](http://www.sciencedirect.com)**ScienceDirect**

Procedia CIRP 86 (2019) 156–161

[www.elsevier.com/locate/procedia](http://www.elsevier.com/locate/procedia)

7th CIRP Global Web Conference

“Towards shifted production value stream patterns through inference of data, models, and technology”

# Method for the Investigation of Mold Filling in the Fiber Injection Molding Process Based on Image Processing

Patrick Moll<sup>a\*</sup>, Axel Schäfer<sup>a</sup>, Sven Coutandin<sup>a</sup>, Jürgen Fleischer<sup>a</sup><sup>a</sup>Karlsruhe Institute of Technology, wbk Institute for Production Science, Kaiserstraße 12, 76131 Karlsruhe, Germany\* Corresponding author. Tel.: +49 1523 9502600; E-mail address: [patrick.moll@kit.edu](mailto:patrick.moll@kit.edu)

## Abstract

Fiber Injection Molding is an innovative process for manufacturing 3D fiber formed parts. Within the process fibers are injected in a special mold through a movable nozzle by an air stream. This process allows a resource efficient production of near net-shape long fiber-preforms without cutting excess. For the properties of the preforms the mold filling is decisive, but current state of the art lacks methods to monitor mold filling online. In this paper a system for monitoring the mold filling based on image processing methods is presented. Therefore a camera and back-lighting has been integrated into a fiber injection mold. The detected filling level and fiber distribution is passed to the PLC of the fiber injection molding machine, which allows the operator to monitor the current mold filling state by means of a visual display. The image processing approach consists of preprocessing, binarization and segmentation. For the preprocessing and binarization several methods including a k-means algorithm, the Otsu thresholding method and a convolutional artificial neural network have been implemented and evaluated. Additionally the illumination of the mold has been investigated and found to have a very large influence on the quality of the results of all investigated methods. The results of the binarization are evaluated on the basis of ground truth images, where an absolute difference between labeled and binarized images is formed and the number of misinterpreted pixels is counted. Among the investigated methods, the method based on the Otsu threshold has been found to be the most efficient with regard to the achievable performance as well as to the correct detection of the current filling. The investigated approach allows the acquisition of more data about the mold filling process to improve models.

© 2019 The Authors. Published by Elsevier B.V.

This is an open access article under the CC BY-NC-ND license (<http://creativecommons.org/licenses/by-nc-nd/4.0/>)

Peer-review under responsibility of the scientific committee of the 7th CIRP Global Web Conference

*Keywords:* Manufacturing Process; Monitoring; Process Control; Mold; Artificial Intelligence

## 1. Introduction

Due to the scarcity of resources and energy, stricter legislation regarding fuel consumption and emissions in the transport sector as well as the growing environmental awareness among the population, the importance of system-efficient lightweight construction has increased significantly in recent years. Research and industry focus on new materials and manufacturing methods to reduce the weight of components [1]. Due to their very good stiffness and strength compared to traditional materials fiber reinforced plastics (FRPs) possess a high potential for

various industry sectors. Other advantageous properties of this material group are its high energy absorption capacity and corrosion resistance.

A major obstacle for the large-scale use of FRPs are the high costs, especially for endless fiber-reinforced components, which results from the higher material and manufacturing costs compared to metallic materials [2].

For semi-structural components and claddings, nonwoven composites represent a cost-efficient alternative to continuous-fiber semi-finished products. In addition to the lower manufacturing costs of nonwovens, this class of semi-finished products is particularly favored by the flexible properties that can be achieved by blending

different fibers, as well as the realization of different fiber structures and a variable isotropy [3]. Additionally, long fiber semi-finished products allow further resource savings and cost reduction through the use of recycled carbon fibers, which have a shorter fiber length of 5-100 mm after the recycling process [3, 4].

In traditional process chains, a fiber preform is manufactured by cutting and stacking pieces from a continuous two-dimensional semi-product. Hence, multiple steps are required and a lot of cutting waste is generated [5]. Direct preforming processes like 3D fiber spraying offer the potential to directly manufacture three-dimensionally shaped preforms with reduced waste [6, 7].

A new alternative process for the direct manufacturing of 3D preforms is the fiber injection molding (FIM) process [8]. The process is suitable to process various fibers like glass and carbon fibers, as well as natural fibers or recycled cutting waste. A thermoplastic bi-component fiber is used to thermobond the fibers. The process has several sequential process steps, which are shown in Fig. 1. In the first step, the fibers are opened in a carding machine and processed to a homogeneous fiber blend with the bi-component fibers. The fiber blend is then blown into a closed, two-part mold, normally made of perforated sheet metal, by means of an air stream. The air can exit through small openings in the mold wall and the fibers are deposited on the inside of the mold. Once the mold has been filled, the upper part of the mold is replaced by another mold and the fiber blank is pressed. During pressing, hot air is blown through the fiber blank, melting the thermoplastic binder fiber and solidifying the fiber blank [8]. On industrial scale the process steps are parallelized in a circular production plant allowing cycle times of 90 s [9].

In addition to the above mentioned advantage of a high material utilization, the geometry variation between injection and compression mold allows the realization of areas with different densities and openings within the final part. In different research projects, the introduction of metallic inserts has been developed and evaluated, allowing a direct load introduction into the fiber structure [10]. For the reinforcement of the long fiber structure the addition of local endless fibers onto a fiber-injection-molded preforms has been evaluated by Dackweiler et al. showing reduction of displacement with a magnitude of 30 % for a medium-

sized part [11].

Besides the advantages of the FIM process there are big fluctuations in the weight of the manufactured preforms and the fiber distribution within the preforms [10, 11]. These fluctuations are due to the formation of bunions during transport of the fibers leading to an uneven filling of the injection mold. As of now, there is no possibility to monitor the filling of the mold without stopping the injection step and opening the mold. To overcome this issue and further investigate the mold filling process, a novel method for the monitoring of the mold is presented in this contribution. The goal is to detect the front of the already injected fibers to display the current mold filling for analysis by the machine operator.

## 2. Modification of injection mold

In other injection or infiltration processes with liquid respectively viscous media the integration of different sensors for process monitoring is considered state of the art. In injection molding it is common since many years to have molds fitted with temperature sensors to survey the cooling rate and pressure sensors to measure the internal mold pressure [12, 13]. These sensors are also used to determine mold filling by detecting the increase of pressure and temperature when the melt front is reaching the sensor. Based on models the injection velocity can be controlled to achieve a constant melt front [14]. Recent research investigates self-optimizing and adaptive control based on sensor data and modeling [15]. For monitoring the resin flow within an RTM mold several sensor types have been investigated. Danisman et al. propose the use of a grid-shaped sensor to measure the resistance and thereby determine mold filling stage [16]. Another approach uses the run time of ultrasonic waves to monitor the curing state of the resin [17]. In series production capacitive sensors to detect the resin flow within the injection mold are used [18].

Due to the low pressure during the injection of the fibers into the mold in the FIM process pressure sensors are not suitable to reliably detect the presence of fibers. The integration of temperature sensors is also not an option, as there is no temperature increase in the injection step. Considering the multitude of different fibers which are

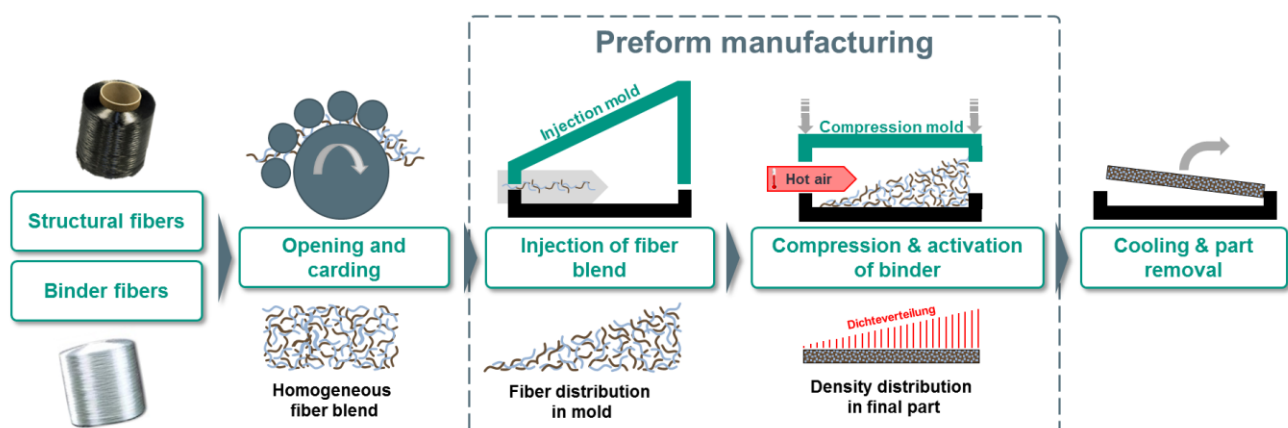


Fig. 1. Process steps of fiber injection molding (FIM) process

processed with very different properties, capacitive and resistive sensors are not suitable to guarantee the detection of the multitude of possible fibers to be processed. Therefore none of the known monitoring solutions from other injection or infiltration processes can be adapted for the FIM process. Additionally, none of these is capable to detect the exact position of the fiber front.

As a result of the shown challenges to detect the fibers within the FIM mold, a new mold was designed to integrate a camera for monitoring the injection process step.

### 2.1. Selection of camera and lens

Before the design of the injection mold the camera and lens for the monitoring system are selected. The combination of camera and lens is required to be able to survey an area of 400 x 400 mm. To detect the injected fibers a high frame rate (> 20 frames per second) is required and the signal-to-noise-ratio should be kept as low as possible. Additionally, hot pixels on the CCD sensor have to be avoided. A further requirement is a resolution of higher than 200 dpi in order to picture the fibers with sufficient precision for further quality control of the finished preforms [19].

To meet the demanded requirements the camera UI-3290SE of the company IDS (Obersulm, Germany) has been selected. With a demanded minimal object distance  $g$  of 300 mm due to limited installation space, the object size  $G$  of 400 mm and the image size  $B$  of 7.5 mm (given by the camera), the required focal distance  $f$  of the lens can be calculated by the following equation:

$$f = \frac{g \cdot B}{G + B} = \frac{300 \text{ mm} \cdot 7.5 \text{ mm}}{400 \text{ mm} + 7.5 \text{ mm}} = 10.84 \text{ mm} \quad (1)$$

The best matching lens for the camera and application is therefore the Tamron M111FM08 with a focal distance of 8 mm.

### 2.2. Design and evaluation of lighting

Due to the darkening of the mold, dedicated lighting of the background is necessary. It must be ensured that the available installation space is limited by the system design. Another important aspect is the spatial and temporal homogeneity of the lighting. It has to be ensured that no flickering occurs on the one hand and that the thresholding methods do not deliver faulty binarization on the other. It is also important that the brightness of the lighting source is dimmable so that the luminous flux can be matched to the aperture opening of the lens to prevent oversaturation of the image sensor avoided.

Based on the requirements shown, it was decided to use commercially available LED strips for the lighting. They can be used very flexibly and offer sufficient homogeneity with careful installation. The LED strips are positioned in an equally spaced linear pattern above the focused object level of the camera.

To evaluate the homogeneity of the lighting the luminosity along a line perpendicular to the LED strip

pattern was evaluated with varying distances between the lighting and the object level. Fig. 2 shows the luminosity along the evaluated line. With a minimal distance of 3 cm the single LED strips are clearly visible. Increasing the distance leads to better homogeneity of the lighting.

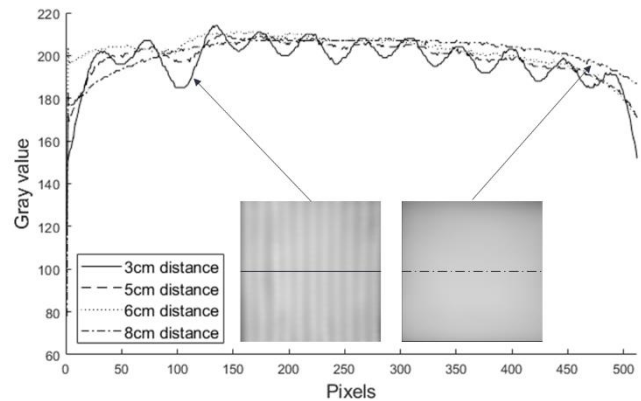


Fig. 2. Evaluation of the background lighting in function of the LED strip distance from the image level

### 2.3. Design of Injection Mold

The injection mold shown in Fig. 3 is designed for a square test part with a dimension of 400 x 400 mm. The side walls of the mold are of perforated sheet metal, as is the case with conventional FIM molds, whereas the bottom and top are made of Plexiglas. Beneath the bottom the camera and lens are placed with a minimum distance of 300 mm. Above the glass top side an additional metal plate is placed in the determined distance of 80 mm, which is equipped with the LED strips to backlight the mold for better detection of the fibers.

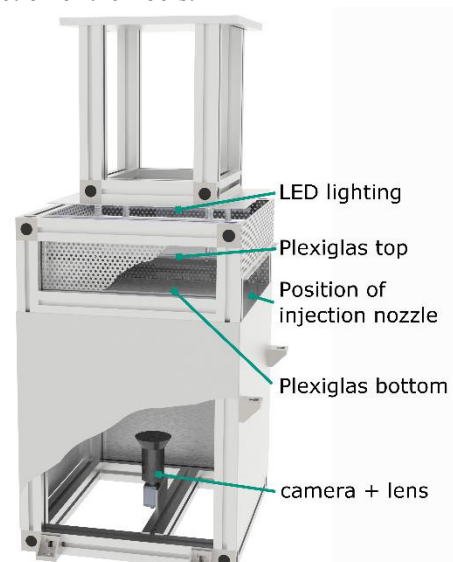


Fig. 3. Components of the mold with integrated camera and lighting

## 3. Image processing

In this section the image processing methods for the extraction of the fiber front from the acquired images are presented. As shown in Fig. 4, the camera is connected to a personal computer via a USB 3 connection. The actual image processing for the extraction of the fiber front runs on the computer with an Intel i5 (2.80 GHz) CPU. Parallel to the image processing a video of the fiber injection process step is saved in a database for later analysis purposes. The result of the image processing program is transferred to the PLC of the fiber injection molding machine in real-time via the Automation Device Specification (ADS) protocol of the PLC manufacturer Beckhoff (Verl, Germany).

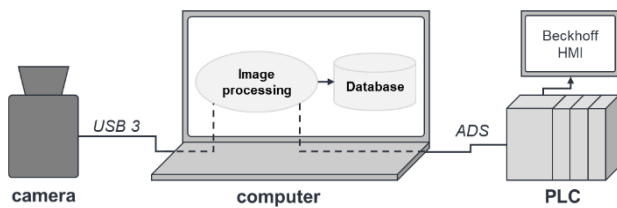


Fig. 4. System architecture of the mold monitoring system

The image processing is realized in the programming language C++ using the free machine vision library OpenCV [20]. The image processing sequence is shown in detail in Fig. 5 and will be described in the following sections.

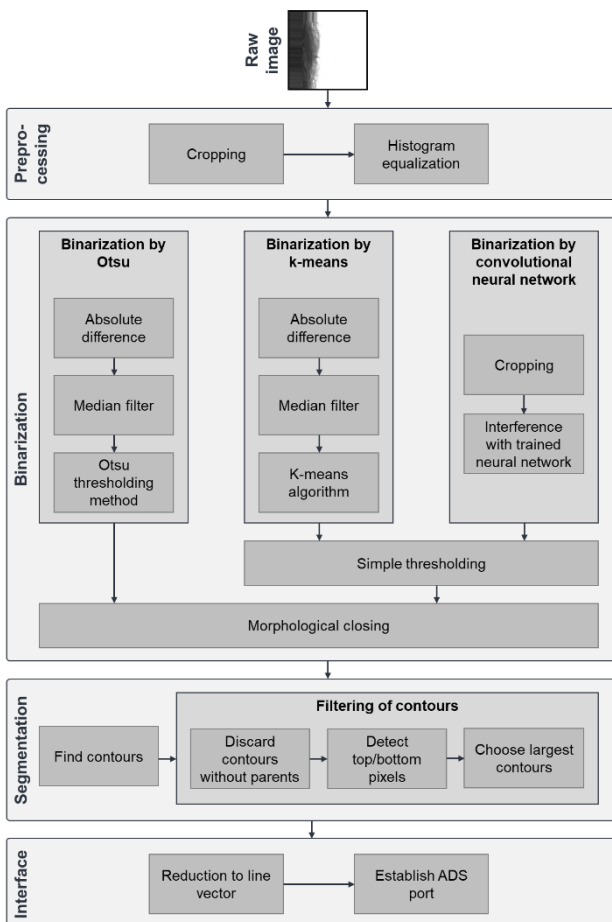


Fig. 5. Sequence of the image processing program

### 3.1. Preprocessing

The images are imported into the program by an interface provided by the manufacturer to directly convert them in the OpenCV image format. During mold filling the images are acquired as gray value images with a resolution of 640 x 450 pixels in order to have less data to process. Since the mold is of squared shape, the images are cropped to meet this format. To remove any deviations caused by the backlighting system the images were normalized by a histogram equalization.

### 3.2. Binarization

The aim of the binarization step is to separate the areas with fibers from the background of the mold. For binarization of the preprocessed images, three different methods are examined in more detail. Subsequently, the suitability of the three methods will be examined and the most efficient method will be used for process monitoring. The three methods are an Otsu thresholding method, a k-means algorithm and a binarization by a convolutional neural network (CNN).

*Otsu thresholding method:* The Otsu thresholding method determines the threshold using the variances in the histogram of the current image [21]. First, the absolute difference of the current image with an image of the empty mold is calculated to eliminate any remaining inhomogeneity due to the illumination. Then a median filter is applied to reduce smaller and individually scattered fibers from the image. Finally, the Otsu thresholding method is applied finishing with a morphological closing operation to minimize small holes in the area where the fibers are located.

*K-means algorithm:* the k-means algorithm is a clustering algorithm for a known number of clusters  $n$ . In the case of binarization the number  $n$  is two and the result equals an image with two distinct gray values. Before applying the algorithm the same absolute difference and median filter as for the Otsu thresholding is applied. Investigations varying the input parameters for the k-means algorithm have shown, that increasing the parameter attempts (specification of the number of times the algorithm is executed using different initial labellings) highly affects the achievable frame rate, whereas the influence of a different value for the number of iterations and the minimum distance for cluster center movement can be neglected. As the result of the k-means algorithm is still a gray value image, it is reduced to a binary image with a simple threshold.

*Convolutional neural network:* For the binarization with a CNN the U-Net architecture developed by Ronneberger et al. is used which is particularly suited for segmentation [22]. It performs very well with little training data at a relatively high speed which is crucial for this near-real-time application. For the training of the CNN 484 images of different video sequences of the injection process have been labeled manually. The architecture of the net and training were performed using Python, whereas the execution for the

binarization purpose was carried out by the C++ program. The applied parameters for the training are shown in Table 1. After each epoch the training images were altered by data augmentation techniques (rotation, sharpening, zooming, translation). For optimization the adaptive moment estimation optimizer (Adam) [23] was used as it turned out to be more performant than the initially used stochastic gradient descent method. As the CNN delivers another gray value image, a further binarization with a simple threshold is performed at the end.

Table 1. Parameters for the training of the U-Net convolutional neural network (CNN)

loss function	binary cross entropy
nb of epochs	20
nb of training images	484
momentum	0.99
learning rate	0.00001
decay	0.000001

After all three methods the binarization finishes with a morphological closing operation to minimize small holes in the area where the fibers are located. In tests an erosion with a circular  $7 \times 7$  pixel element and a dilation with an  $11 \times 11$  pixel element was found out to be the best compromise between achievable frame rate and accuracy of the edge between the black and white phase.

### 3.3. Segmentation

The segmentation step is intended to convert the information of the binarized image into a boundary line representing the front of the injected fibers. For the detection of the boundary line the *findContours* algorithm from the OpenCV library is used.

Since several contours can be found depending on the binarization results, the contour that represents the fiber front must be identified in a three step filter process. For this purpose, all contours that are within another contour (child contours) are discarded first. Only the remaining contours possessing no parent contours on their own can be parent contours. The relevant contours must always have pixels at the top and bottom, which is checked in a second filter step. The last filter to be selected is the largest remaining contour. This contour is the target contour which represents the fiber front.

### 3.4. Interface to machine controller

For the transfer to the machine PLC the contour from the segmentation step is reduced to a line vector with the coordinates of the fiber front at discrete equidistant positions, which represents the position of the fiber front. Via the Beckhoff ADS protocol the line vector can be transferred from the C++ program to the real-time kernel on the PLC. The visualization of the fiber front is performed with a line chart by the Beckhoff human machine interface.

## 4. Results and Discussion

Fig. 6 contains images of the filling state inside the mold taken by the integrated camera at different times of the injection process step. The different lines shown in the images represent the position of the fiber front detected by the image processing program with the presented three different binarization approaches.

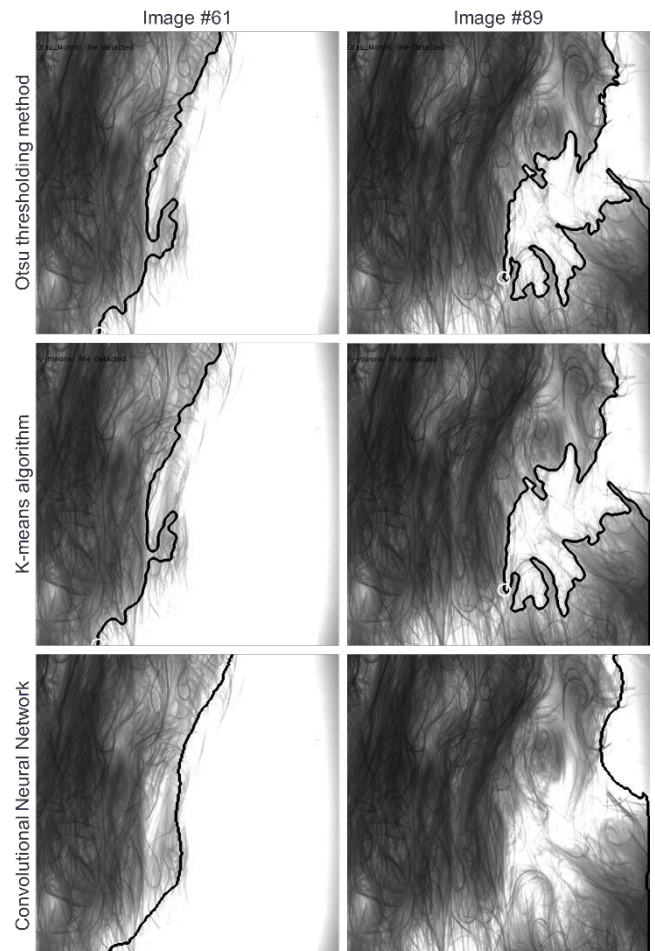


Fig. 6. Images of the mold filling at different states of the injection process step with the detected fiber front

It is obvious that the binarization step is crucial for the result of the fiber front detection as it separates the areas with fibers from the background. Therefore the result of the binarization was evaluated specifically using the pixel error between the output images of the binarization step after morphological closing and a hand-labeled ground-truth image.

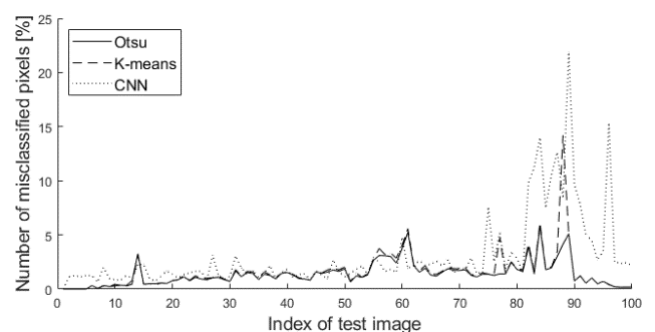


Fig. 7. Error of the different binarization methods

Fig. 7 represents the error of the different methods applied to 100 images in chronological order of the mold filling process step. Table 2 shows the average and maximum error of the methods. The CNN has the worst performance mainly due to bad binarization results at the end of the injection process. The other two investigated methods have a similar performance with an average error around 1.5 % and a maximum error of 5.25 % in the case of the Otsu thresholding method, which is sufficient for the purpose of mold filling monitoring.

Table 2. Average and maximum error of the implemented binarization methods

binarization method	average error	max. error
Otsu thresholding method	1.40 %	5.25 %
k-means algorithm	1.61 %	14.17 %
convolutional neural network	3.01 %	21.85 %

In terms of performance the proposed methods differ a lot. With the Otsu method a frame rate of 7 frames per second (fps) is achieved computing on the main processor of the used computer. With the k-means algorithm a frame rate of 1.5 fps respectively 0.5 fps for the CNN can be achieved.

## 5. Summary and outlook

This paper outlines a new approach for the monitoring of mold filling in fiber injection molding. The images of a mold-integrated camera are processed in a computer using the OpenCV library to detect the front of the injected fibers. It has been shown, that binarization of the images poses the biggest challenge with the best results regarding error rate and performance achieved by the Otsu thresholding method. For the detection of the fiber front, the *findContours* function of OpenCV was used. The position of the fiber front is then transferred to the machine PLC for visualization on the human machine interface.

In ongoing research the position of the fiber front is used for the adaptive control of the fiber injection nozzle with the goal of improving the uniformity of the manufactured fiber preforms. Additionally, a high-resolution image of the injected fibers captured by the mold-integrated camera at the end of the injection process step are used for an online quality control. The algorithms used to compute the uniformity and fiber orientation distribution will be outlined in a future paper. Additionally the detection reliability for other types of fibers, e.g. carbon fibers, has to be evaluated thoroughly. As other fibers are more opaque compared to glass fibers, the results for other fibers are expected to be good.

## Acknowledgement

This work was supported by a grant from the State ministry of Science, Research and the Arts of Baden-Württemberg to Mr. Jürgen Fleischer.

## References

- [1] Taub, A.I., Luo, A.A., 2015. Advanced lightweight materials and manufacturing processes for automotive applications 40, p. 1045.
- [2] Fleischer, J., Teti, R., Lanza, G., Mativenga, P. et al., 2018. Composite materials parts manufacturing 67, p. 603.
- [3] Steguschter, G., Schlichter, S., 2018. Perspectives of web based composites from RCF material 406, p. 12022.
- [4] Wölling, J., Schmieg, M., Manis, F., Drechsler, K., 2017. Nonwovens from Recycled Carbon Fibres – Comparison of Processing Technologies 66, p. 271.
- [5] Fleischer, J., Lanza, G., Brabandt, D., Wagner, H., 2012. Overcoming the challenges of automated pre-forming of semi-finished textiles, in Symposium on Automation of Advanced Composites and its Technology.
- [6] Harper, L.T., 2006. Discontinuous carbon fibre composites for automotive applications.
- [7] Böttcher, A., Pöhler, M., Rösner, A., Engelmann, C. et al., 2012. New Process Chain for Fiber Reinforced Lightweight Components, p. 36.
- [8] Förster, E. Verfahren und Vorrichtung zur Herstellung von dreidimensional ausgeprägten Formteilen sowie Formteil, 2003(DE 103 24 735 B3).
- [9] Förster, E., 2015. Ressourceneffizienz mit FIM zur Fertigung von 3D-Faserformteilen 23, p. 103.
- [10] Dackweiler, M., Fleischer, J., 2015. Herstellung intrinsisch hybrider Bauteile: Herausforderungen zukünftiger Fertigungsprozesse am Beispiel des Faserblasverfahrens, in Serienfertigung mit unreifen Prozessen: Tagungsband zur wbk Herbsttagung 2015, Shaker Verlag, Aachen, p. 79.
- [11] Dackweiler, M., Fleischer, J., 2017. Automated local reinforcing of glass fiber-injection-molded preforms with carbon fiber tapes, in Proceedings of the 15th Japan International SAMPE Symposium&Exhibition.
- [12] Agrawal, A.R., Pandelidis, I.O., Pecht, M., 1987. Injection-molding process control?A review 27, p. 1345.
- [13] Chen, Z., Turng, L.-S., 2005. A review of current developments in process and quality control for injection molding 24, p. 165.
- [14] Chen, X., Gao, F., 2006. Profiling of injection velocity for uniform mold filling 25, p. 13.
- [15] Hopmann, C., Abel, D., Heinisch, J., Stemmler, S., 2017. Self-optimizing injection molding based on iterative learning cavity pressure control 11, p. 97.
- [16] Danisman, M., Tuncol, G., Kaynar, A., Sozer, E.M., 2007. Monitoring of resin flow in the resin transfer molding (RTM) process using point-voltage sensors 67, p. 367.
- [17] Berger, D., Zaiß, M., Lanza, G., Summa, J. et al., 2018. Predictive quality control of hybrid metal-CFRP components using information fusion 12, p. 161.
- [18] Arnold, M., Franz, H., Bobertag, M., Glück, J. et al., 2013. Kapazitive Messtechnik zur RTM-Prozessüberwachung, p. 50.
- [19] Amimasr, E., Shim, E., Yeom, B.-Y., Pourdeyhimi, B., 2014. Basis weight uniformity analysis in nonwovens 105, p. 444.
- [20] Bradski, G., 2000. The OpenCV Library.
- [21] Otsu, N., 1979. A Threshold Selection Method from Gray-Level Histograms 9, p. 62.
- [22] Ronneberger, O., Fischer, P., Brox, T., 2015. U-Net: Convolutional Networks for Biomedical Image Segmentation, in Medical image computing and computer-assisted intervention - MICCAI 2015: 18th international conference, Munich, Germany, October 5-9, 2015; proceedings, Springer, Cham, p. 234.
- [23] Kingma, D.P., Ba, J., 2014. Adam: A Method for Stochastic Optimization.